FACTA UNIVERSITATIS
Series: **Mechanics, Automatic Control and Robotics** Vol.3, Nº 11, 2001, pp. 37 - 53

COMPUTATATION OF INCOMPRESSIBLE TURBULENT BOUNDARY LAYER WITH FAVORABLE AND ADVERSE PRESSURE GRADIENT AT HIGH REYNOLDS NUMBERS

UDC 532.517.4:532.526

Miloš M. Jovanović

University of Niš, Faculty of Mechanical Engineering, Beogradska 14, 18000 Niš
Serbia, Yugoslavia

Abstract. *It is shown that the turbulent boundary layer consists of two layers: the fully turbulent layer (defect layer) and the viscous wall layer. The calculation can be restricted to the fully turbulent layer (defect layer), whose equations are independent of Reynolds number. The corresponding boundary conditions follow from the matching with the inviscid outer flow (at the outer edge $y = \delta$) and with the viscous wall layer flow (at the overlap layer $y \approx \delta_v$) respectively. The structure of the skin friction law is independent of the turbulence model. Three algebraic models have been used in the calculation of the defect layer global values. The velocity and stress distribution within viscous wall layer at high Reynolds number have universal form, if the Reynolds number is high enough ($Re_\theta > 6000$).*
In this way, at the given potential flow velocity distribution on the outer edge of boundary layer, it is only needed one calculation to be carried out. The influence of the Reynolds number is taken into account only for the calculation of local skin friction, which follows from matching conditions to the wall layer flow, better to say, to the universal logarithmic wall layer law. The global characteristics of turbulent boundary layer can be obtained by the numerical solution of the governing equation over the defect layer of turbulent boundary layer.

1. INTRODUCTION

The primary emphasis in this paper is upon the large Reynolds number asymptotic theory of turbulent boundary layers. The origin of this approach dates back to the paper of Mellor (1972), where he has shown that the flow field near the wall at high Reynolds numbers has three distinctive areas with different time and length scales: outer inviscid flow, fully turbulent defect layer, and viscous wall layer.

This method has been recently extended in the paper of Gersten (1995) where the author explained two version of this method: integral approach and differential approach. The second one has been used in this paper.

Received October 5, 2000

The main goal of this paper was to test three different algebraic turbulent models, which are mostly used in engineering practice, and to compare the results that are obtained with the available experimental data, and to estimate which one best fits the experimental results.

At high Reynolds numbers the flow field consists of an inviscid outer flow and of the boundary layer. When the Reynolds number is high enough the flow in the boundary layer is turbulent. The turbulent boundary layer has two new features compared to the laminar one. First, it has distinctive outer edge with the wall distance (or boundary layer thickness) δ as shown in the Fig. 1.1. This outer edge separates the inviscid nonturbulent outer flow from the turbulent boundary-layer flow. Second, the turbulent boundary layer consists of two layers, the fully turbulent outer part, where viscosity effects are negligible and the viscous wall layer, where viscosity effects have to be taken into account. The thickness of the viscous wall layer is $\delta_v(x)$. Both thickness $\delta(x)$ and $\delta_v(x)$ tend to zero for increasing Reynolds number, but $\delta_v(x)$ decreases much faster than $\delta(x)$. As it will be shown later the viscous wall layer is governed by universal laws which are determined mainly by viscosity and the wall shear stress. From the asymptotic theory for high Reynolds numbers it can be concluded, that for a given pressure distribution only the flow in the fully turbulent outer part of the boundary layer (defect layer) has to be calculated. The flow equations valid for this fully turbulent layer become independent of Reynolds number. The corresponding boundary conditions follow from the matching with the inviscid outer flow (at the outer edge $y = \delta$) and with the viscous wall layer (at the overlap layer $y \approx \delta_v$) respectively.

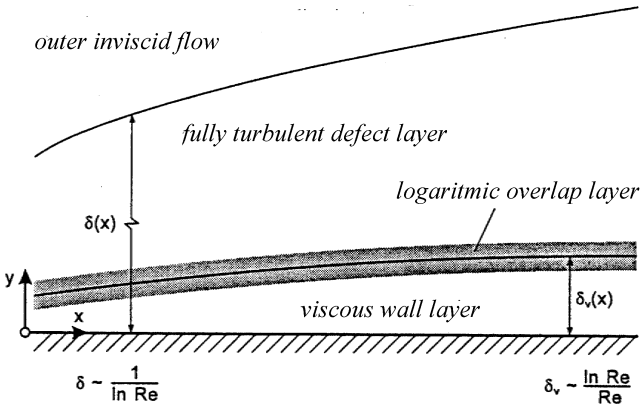

Fig. 1.1. Layer structure of turbulent boundary layers

2. VISCOUS WALL LAYER

In this paper the two-dimensional, steady, turbulent boundary layer flows with constant properties have been considered. The following equations have been obtained by time averaging for this flow:

$$\rho\left(\overline{U}\frac{\partial\overline{U}}{\partial x}+\overline{V}\frac{\partial\overline{U}}{\partial y}\right)=-\frac{\partial p_e}{\partial x}+\frac{\partial}{\partial y}(\overline{\tau}_v+\tau_t)\,, \tag{2.1}$$

$$\frac{\partial \overline{U}}{\partial x}+\frac{\partial \overline{V}}{\partial y}=0\,, \tag{2.2}$$

where are, $\overline{U}(x,y),\overline{V}(x,y)$ - streamwise and cross-stream time averaged velocity respectively, ρ - fluid density, $\tau_v(y)$, $\tau_t(x,y)$ - viscous and turbulent shear stress respectively, x, y - streamwise and cross-stream (normal) coordinate respectively and $p_e(x)$ - pressure at the outer edge of turbulent boundary layer, and according to the first order boundary layer theory, see Mellor (1972), is independent of coordinate y, where the expressions for viscous and turbulent shear stress read,

$$\tau_v=\mu\frac{\partial \overline{U}}{\partial y}\,,\qquad \tau_t=-\rho\overline{u'\upsilon'}\,. \tag{2.3}$$

To describe the very thin viscous wall layer the following normal coordinate is used:

$$y^+=\frac{u_\tau(x)y}{\nu}\,,\quad u_\tau^2(x)=\frac{\overline{\tau}_w(x)}{\rho}\,, \tag{2.4}$$

where u_τ - *friction velocity*, $\overline{\tau}_w$ - *wall shear stress,* ν - *kinematic fluid viscosity*. When the variables are nondimensionalised by

$$\begin{gathered} x^*=\frac{x}{L}\,,\qquad \mathrm{Re}=\frac{U_\infty L}{\nu}\,,\quad u_\tau^*=\frac{u_\tau}{U_\infty}\,,\quad p_e^*=\frac{p_e-p_\infty}{\rho U_\infty^2}\,,\\ u^+=\frac{\overline{U}}{u_\tau}\,,\qquad v^+=\frac{\overline{V}}{u_\tau}\,,\qquad \tau^+=\frac{\overline{\tau}_v+\tau_t}{\rho u_\tau^2}\,. \end{gathered} \tag{2.5}$$

U_∞ and p_∞ are the velocity and pressure of the undisturbed incoming flow, L - streamwise length scale, u^+,v^+ - dimensionless streamwise and cross-stream velocity, and τ^+ - dimensionless total shear stress. The Reynolds-averaged flow equations reduce to

$$\frac{1}{\mathrm{Re}u_\tau^*}\left(\frac{u^{+2}}{u_\tau^*}\frac{\partial u_\tau^*}{\partial x^*}+u^+\frac{\partial u^+}{\partial x^*}+\frac{1}{u_\tau^{*2}}\frac{dp_e^*}{dx^*}\right)+v^+\frac{\partial u^+}{\partial y^+}=\frac{\partial \tau^+}{\partial y^+}\,, \tag{2.6}$$

$$\frac{1}{\mathrm{Re}u_\tau^*}\left(\frac{u^+}{u_\tau^*}\frac{\partial u_\tau^*}{\partial x^*}+\frac{\partial u^+}{\partial x^*}\right)+\frac{\partial V^+}{\partial y^+}=0\,. \tag{2.7}$$

For the limit $\mathrm{Re}u_\tau^*\to\infty$ these equations have solution:

$$v^+=0,\quad \tau^+=const=1\,. \tag{2.8}$$

The expression within the brackets in Eq.(2.7) tends to zero for high Reynolds numbers so that we have that $\partial v^+/\partial y^+\to 0$, and having in mind no-slip wall condition $v^+(y^+=0)=0$, it is obvious that the normal velocity in viscous wall layer is zero. Its now evident that last term on the left-hand side of the Eq.(2.6) is also zero for high Reynolds numbers, so that we have now $\partial\tau^+/\partial y^+\to 0$. The attached flow in the wall layer is independent of pressure gradient, and the sum of viscous and turbulent shear stress is constant.

In the overlap layer we have

$$\tau_t = \tau_w + \frac{dp}{dx} = \tau_w \left[1 + \frac{dp^*}{dx^*} \frac{1}{\mathrm{Re}\, u_\tau^{*3}} y^* \right] \approx \tau_w \,, \tag{2.9}$$

Since the overlap layer must have the features of both adjacent layers, its flow field is (as part of the fully turbulent layer) independent of the viscosity and (as part of the viscous wall layer) independent of boundary layer thickness δ. Hence, the following relationship between the turbulent shear stress $\tau_t = -\rho\overline{u'v'}$ and the velocity gradient $\partial\overline{U}/\partial y$ must be valid in the overlap layer

$$f\left(\frac{\partial \overline{U}}{\partial y}, y, \frac{\tau_t}{\rho} \right) = 0. \tag{2.10}$$

Applying the π-theorem of dimensional analysis leads to the overlap law:

$$\lim_{y \to \infty} \frac{y}{\sqrt{\tau_t / \rho}} \frac{d\overline{U}}{dy} = \frac{1}{\kappa} \quad , \tag{2.11}$$

where κ is the *Karman constant*. According to Eq.(11) we have

$$\lim_{y^+ \to \infty} \frac{du^+}{dy^+} = \frac{1}{\kappa y^+} , \tag{2.12}$$

which leads to the well known *universal logarithmic law*

$$\lim_{y^+ \to \infty} u^+ = \frac{1}{\kappa} \ln y^+ + C^+ , \tag{2.13}$$

with the integration constant C^+. This constant is $C^+ = 5.0$ for smooth walls and a well-known function of the dimensionless roughness parameter $k^+ = k u_\tau / \nu$ for rough walls, respectively.

On the basis of the analysis carried out in Jovanovic (1998), the function which should represent the velocity distribution in viscous wall layer, has to satisfy the following asymptotic conditions

$$y^+ \to 0: \qquad \frac{du^+}{dy^+} = 1 - A y^{+3}, \qquad u^+ = y^+ - \frac{A}{4} y^{+4}, \tag{2.14}$$

$$y^+ \to \infty: \qquad \frac{du^+}{dy^+} = \frac{1}{\kappa y^+}, \qquad u^+ = \frac{1}{\kappa} \ln y^+ + C^+. \tag{2.15}$$

The expression for the first derivation of the function which is looked for, and which satisfies these boundary conditions, reads

$$\frac{du^+}{dy^+} = f'(y^+) = \frac{1}{1 + (A+B) y^{+3}} + \frac{B y^{+3}}{1 + \kappa B y^{+4}} \tag{2.16}$$

By the integration of the Eq.(2.16), where it have been taken in account that $u^+(0) = 0$, the following function is obtained

$$u^+ = \frac{1}{3\lambda}\left[\ln\frac{\lambda y^+ + 1}{\sqrt{(\lambda y^+)^2 - \lambda y^+ + 1}} + \sqrt{3}\left(arctg\ \ \frac{2\lambda y^+ - 1}{\sqrt{3}} + \frac{\pi}{6}\right)\right] + \frac{\ln(1 + \kappa B y^{+4})}{4\kappa}. \quad (2.17)$$

where the following constants have been used

$$\kappa = 0.41, \quad A = 6.1\cdot 10^{-4}, \quad B = 1.43\cdot 10^{-3}, \quad \lambda = \sqrt[3]{A + B}. \quad (2.18)$$

Having in mind the expression for nondimensional total shear stress in viscous wall layer in Eq.(2.5) and the conclusion that have been drawn for the case of $\mathrm{Re}u_\tau^* \to \infty$ Eq.(2.8), the following equality can be written for the case of high Reynolds numbers

$$\tau_w = \overline{\tau}_v + \tau_t = \mu\frac{d\overline{U}}{dy} - \rho\overline{u'\upsilon'} = const. \quad (2.19)$$

If the equation Eq.(2.19) is divided by fluid density ρ which is constant for incompressible, isothermal flow, the Eq.(2.19) now reads

$$u_\tau^2 = \nu\frac{d\overline{U}}{dy} - \overline{u'\upsilon'}. \quad (2.20)$$

If the Eq.(2.20) is divided by u_τ^2, this equation yields now

$$1 = \frac{d(\overline{U}/u_\tau)}{d(yu_\tau/\nu)} - \frac{\overline{u'v'}}{u_\tau^2} = \frac{du^+}{dy^+} + \frac{\tau_t}{\tau_w} = \frac{du^+}{dy^+} + \tau_t^+. \quad (2.21)$$

The nondimensional turbulent shear stress in viscous wall layer now reads

$$\tau_t^+ = 1 - \frac{du^+}{dy^+} \quad (2.22)$$

If the Eq.(2.16) is substituted in the (2.22), the nondimensional turbulent shear stress distribution obtains the universal form. In the Fig.2.1 are shown the nondimensional turbulent shear stress and nondimensional velocity distribution in viscous wall layer according to the Eq.(2.16), (2.17) and (2.22).

From the Fig.2.1 we see that the velocity distribution in the viscous wall layer rises from no-slip at the wall and obeys the asymptotic conditions (2.14) and merges smoothly at $y^+ \approx 70$ with the overlap logarithmic law. The velocity distribution between the asymptotics given by (2.14) and (2.15) is described by the function (2.17).

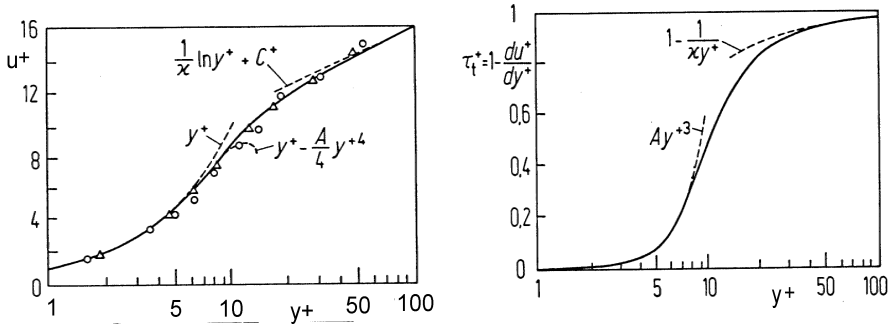

Fig. 2.1. Velocity and turbulent stress distribution in viscous wall layer

The viscous stress is dominant in the region $y^+ < 5$, and this part of viscous wall layer is known as *viscous sublayer*. In this point the participation of viscous stress is about 95% of the total shear stress, and at the value $y^+ \approx 10$ the contribution of viscous and turbulent stress to the total shear stress are equals. From this point the participation of viscous part decreases rapidly, so that the beyond the point $y^+ = 50$ the influence of the viscous stress is significantly reduced. For the values $y^+ > 100$ viscous stress practically can be neglected. Therefore it is avoided to calculate the whole viscous wall layer which is anyhow universal and hence known a priori for a given wall shear stress.

3. FULLY TURBULENT LAYER (DEFECT LAYER)

The momentum and continuity equations of this part of turbulent boundary layer read

$$\rho\left(\overline{U}\frac{\partial \overline{U}}{\partial x} + \overline{V}\frac{\partial \overline{U}}{\partial y}\right) = -\frac{\partial p_e}{\partial x} + \frac{\partial \tau_t}{\partial y}, \tag{3.1}$$

$$\frac{\partial \overline{U}}{\partial x} + \frac{\partial \overline{V}}{\partial y} = 0. \tag{3.2}$$

The flow field for high Reynolds numbers is calculated in two steps. In the first step the inviscid outer flow is determined usually by the methods of potential theory. The resulting pressure distribution (or velocity distribution $U_e(x)$) is input for calculating the fully turbulent layer . For this layer the following form of the solution is assumed:

$$\overline{U}(x,y) = U_e(x) - u_\tau(x)F'(x,\eta) = U_e(x)[1-\gamma(x)F'(x,\eta)], \tag{3.3}$$

$$\overline{V} = u_\tau\left[\frac{\partial F}{\partial x}\delta + (F-\eta F')\frac{d}{d}\frac{\delta}{x} + \frac{\delta}{u_\tau}\left(\frac{du_\tau}{dx}F - \frac{dU_e}{dx}\eta\right)\right], \tag{3.4}$$

$$\tau_t = -\rho\overline{u'v'} = \rho u_\tau^2(x)S(x,\eta) = \rho U_e^2(x)\gamma^2(x)S(x,\eta)\ , \tag{3.5}$$

$$p_e - p_\infty = \frac{\rho}{2}U_\infty^2\left(1 - \frac{U_e^2}{U_\infty^2}\right), \tag{3.6}$$

$$\gamma(x)=\frac{u_\tau(x)}{U_e(x)}\ ,\ F'(x,\eta)=\frac{\partial F(x,\eta)}{\partial\eta},\quad \eta=\frac{y}{\delta(x)},\quad u_\tau(x)=\sqrt{\frac{\tau_w}{\rho}}. \tag{3.7}$$

The primes refer to derivatives with respect to η. $U_e(x)$ and $p_e(x)$ are the velocity and pressure at the edge of boundary layer and U_∞ is the velocity of the undisturbed incoming flow. The equation (3.3-3.7) can be considered as perturbation of the limiting solution $\overline{U}(x,y)=U_e(x)$ for $Re=\infty$, where $\gamma(x)$ works as perturbation parameter. Since $F'(x,\eta)$ represents the dimensionless velocity defect, this fully turbulent layer is also called *defect layer* (for attached flows, $\tau_w\neq 0$). As will be shown later, see Eq.(3.26), it is $\delta/L=O(\gamma)=O(1/\ln Re)$. Hence the limit $\gamma(x)\to 0$ is equivalent to the limit $Re\to\infty$. When Eqs. (3.3−3.7) are introduced into the Reynolds-averaged Navier-Stokes equations, the momentum equation for the x-direction yields,

$$\begin{aligned}&\frac{1}{u_\tau}\eta F''\frac{d(U_e\delta)}{dx}-\frac{\delta}{u_\tau^2}\frac{d(U_e u_\tau)}{dx}F'+\frac{\delta}{u_\tau}\frac{du_\tau}{dx}F'^2-\frac{1}{u_\tau}\frac{d(u_\tau\delta)}{dx}F''F=\\&\quad=F''\frac{\partial F}{\partial x}\delta+\frac{\partial F'}{\partial x}\left(\frac{U_e\delta}{u_\tau}-\delta F'\right)+S'.\end{aligned} \tag{3.8}$$

The equation above is dimensionless momentum equation of defect layer. It is partial nonlinear differential equation of second order. This equation can be simplified by the substitution of the dimensional values by the corresponding nondimensional values

$$x=l_R x^*,\quad U_e=U_R U_e^*,\quad u_\tau=\frac{U_R}{\ln \mathrm{Re}}u_\tau^*,\qquad \delta=\frac{l_R}{\ln \mathrm{Re}}\delta^*, \tag{3.9}$$

where U_R and l_R are the reference velocity and length scales, respectively. By substituting the dimensional values with nondimensional ones (3.9) in the equation (3.8), this equation reads

$$\begin{aligned}&\frac{1}{u_\tau^*}\frac{d(U_e^*\delta^*)}{dx^*}\eta F''-\frac{\delta^*}{u_\tau^{*2}}\frac{d(U_e^*u_\tau^*)}{dx^*}F'+\frac{1}{\ln \mathrm{Re}}\frac{\delta^*}{u_\tau^*}\frac{du_\tau^*}{dx^*}F'^2-\frac{1}{\ln \mathrm{Re}}\frac{1}{u_\tau^*}\frac{d(u_\tau^*\delta^*)}{dx^*}F''F=\\&\quad=\frac{1}{\ln \mathrm{Re}}F''\frac{\partial F}{\partial x^*}\delta^*+\frac{\partial F'}{\partial x^*}\left(\frac{U_e^*\delta^*}{u_\tau^*}-\delta^*F'\frac{1}{\ln \mathrm{Re}}\right)+S'.\end{aligned} \tag{3.10}$$

This equation is reduced in the limit $Re\to\infty$, $\gamma(x)\to 0$ to the following defect-layer equation

$$A(x^*)\eta F''+B(x^*)F'-S'=\frac{\partial F'}{\partial x^*}\widetilde{\Delta}(x^*), \tag{3.11}$$

where the following expressions have been introduced

$$A(x^*)=\frac{d\widetilde{\Delta}}{dx^*}+\frac{\widetilde{\Delta}}{U_e}\frac{dU_e}{dx^*}\ ,\ B(x^*)=-\frac{2\widetilde{\Delta}}{U_e}\frac{dU_e}{dx^*}, \tag{3.12}$$

$$\widetilde{\Delta}(x^*)=\frac{U_e\delta}{u_\tau l_R}=\frac{\delta}{\gamma l_R}. \tag{3.13}$$

The boundary conditions are:

$$\lim_{\eta\to 0} F = 0, \quad \lim_{\eta\to 0} F'' = -\frac{1}{\kappa\eta}, \quad \lim_{\eta\to 0} S = 1, \qquad \eta = 1: \quad F' = 0, \quad S = 0. \tag{3.14}$$

The conditions for $\eta \to 0$ are the matching conditions, in the overlap layer. The formulation of the boundary-layer problem by Eqs.(3.11) to (3.14) is called the *method of wall functions*. It uses the matching condition in the overlap layer as boundary condition rather than the conditions directly to the wall (e.g.: no-slip condition). Integration of Eq.(6) over the defect layer yields

$$\frac{d(F_e\tilde{\Delta})}{dx^*} + \frac{3}{U_e}\frac{dU_e}{dx^*}F_e\tilde{\Delta} = 1, \tag{3.15}$$

with the solution

$$\hat{\Delta} = \tilde{\Delta}F_e = \frac{C + \int U_e^3 dx^*}{U_e^3}, \tag{3.16}$$

where is $F_e = F(x,\eta = 1)$. From the solution $F(x,\eta)$ the following global values can be determined:

Boundary value: $$F_e = F(x,1) = \frac{\delta_1}{\delta\gamma}, \tag{3.17}$$

Wake parameter: $$\Pi(x^*) = \frac{\kappa}{2}\lim_{\eta\to 0}\left[F'(x^*,\eta) + \frac{1}{\kappa}\ln\eta\right], \tag{3.18}$$

Shape parameter: $$G(x^*) = \frac{\lim\limits_{y\to 0}\int\limits_y^\delta (U_e - \overline{U})^2 dy}{\lim\limits_{y\to 0}\int\limits_y^\delta (U_e - \overline{U}) dy} = \frac{1}{F_e}\lim_{\eta\to 0}\int_\eta^1 F'^2 d\eta. \tag{3.19}$$

All the global values are, as already mentioned, independent of Reynolds number as well as independent of wall roughness k^+. Eventually these parameters come into the picture, when the wall-shear-stress or the function $\gamma(x) = \sqrt{c_f(x)/2}$ have to be determined. The matching condition in the overlap layer

$$\lim_{y\to 0}\frac{\overline{U}(x,y)}{u_\tau(x)} = \lim_{y^+\to\infty} u^+(y^+) = \frac{1}{\kappa}\ln y^+ + C^+ \ , \tag{3.20}$$

yields according to Eqs.(2.13) and (3.3)

$$\frac{U_e(x,y)}{u_\tau(x)} - \lim_{\eta\to 0} F'(x^*,\eta) = \frac{1}{\kappa}\ln\frac{y u_\tau}{\nu} + C^+ \ . \tag{3.21}$$

If the function $F'(x^*,\eta)$ is expressed by the equation (3.18), the Eq(3.21) reads

$$\frac{1}{\gamma(x)} = \frac{U_e(x,y)}{u_\tau(x)} = \frac{1}{\kappa}\ln\frac{\delta u_\tau}{\nu} + C^+ + \frac{2\Pi(x^*)}{\kappa} \ . \tag{3.22}$$

If the same term is added and subtract to the right-hand side of the Eq.(3.22)

$$\frac{1}{\gamma(x)}=\frac{U_e(x,y)}{u_\tau(x)}=\frac{1}{\kappa}\ln\frac{\delta u_\tau}{\nu}-\frac{1}{\kappa}\ln\left[\frac{U_e}{U_R}\tilde{\Delta}(x^*)\right]+C^+ +\frac{2\Pi(x^*)}{\kappa}+\frac{1}{\kappa}\ln\left[\frac{U_e}{U_R}\tilde{\Delta}(x^*)\right], \qquad (3.23)$$

and if these terms are rearranged and taking into account the Eq.(3.13), the equation (3.23) obtains the new form

$$\frac{1}{\gamma}=\frac{1}{\kappa}\ln(\gamma^2\,\mathrm{Re})+C^+ +\tilde{C}(x^*), \qquad (3.24)$$

where the function $\tilde{C}(x^*)$ is defined by the following expression

$$\tilde{C}(x^*)=\frac{1}{\kappa}\left[2\Pi\left(x^*\right)+\ln\left\{\frac{U_e(x^*)}{U_R}\tilde{\Delta}(x^*)\right\}\right]. \qquad (3.25)$$

Eq.(3.24) for the function $\gamma(x)$ can be written as an explicit skin-friction law

$$\gamma=\frac{u_\tau}{U_e}=\sqrt{\frac{c_f}{2}}=\frac{\kappa}{\ln\mathrm{Re}}G(\Lambda;D), \qquad (3.26)$$

were the function $G(\Lambda;D)$ is defined as

$$\frac{\Lambda}{G}+2\ln\frac{\Lambda}{G}-D=\Lambda;\quad \Lambda=\ln\mathrm{Re};\quad D(x^*)=2\ln\kappa+\kappa[C^+ +\tilde{C}(x^*)]. \qquad (3.27)$$

this function can be expressed in the explicit form by asymptotic expansion

$$G(\Lambda;D)=\left[1-\frac{2\ln\Lambda-D}{\Lambda}\left(1-\frac{2}{\Lambda}\right)\right]^{-1}\qquad \Lambda\to\infty. \qquad (3.26)$$

The three turbulent algebraic models have been used in calculation, Cebecci-Smith (1974)

$$S(x,\eta)=\frac{\nu_t}{u_\tau^2}\frac{\partial\overline{U}}{\partial y}=\frac{\alpha U_e\delta_1}{u_\tau^2(1+5{,}5\eta^6)}\frac{\partial\overline{U}}{\partial y}=\frac{\alpha F_e F''}{1+5{,}5\eta^6}, \qquad (3.28)$$

where is $\alpha = 0.016$. Michell (1968) model yields

$$S(x,\eta)=\frac{\nu_t}{u_\tau^2}\frac{\partial\overline{U}}{\partial y}=\frac{\nu_t}{u_\tau\delta}F''=\frac{\ell^2}{u_\tau\delta}\left|\frac{\partial\overline{U}}{\partial y}\right|F''=\frac{\ell^2}{u_\tau\delta}\frac{u_\tau}{\delta}F''^2=\frac{\ell^2}{\delta^2}F''^2\ . \qquad (3.29)$$

Substituting the expression for mixing length suggested by Michel into (3.29),

$$S(x,\eta)=\frac{\ell^2}{\delta^2}F''^2=\frac{\delta^2c^2}{\delta^2}\tanh\left(\frac{\kappa}{c}\eta\right)F''^2=c^2\tanh\left(\frac{\kappa}{c}\eta\right)F''^2. \qquad (3.30)$$

where $c = 0.085$, and $\kappa = 0.41$. If $\eta > 0.6$, the mixing length is practically independent of η

$\ell \approx c\delta(x)$ and the nondimensional turbulent stress have the form

$$S(x,\eta) = \frac{\ell^2}{\delta^2} F''^2 = \frac{c^2\delta^2}{\delta^2} F''^2 = c^2 F''^2. \tag{3.31}$$

The Clauser (1956) model gives the following expression for turbulent stress

$$S(x,\eta) = \frac{\nu_t}{u_\tau \delta} F'' = \frac{\alpha U_e \delta_1}{u_\tau \delta} F'' = \alpha F_e F''. \tag{3.32}$$

For the comparison of the calculation results with the existing experimental data, the flows, which are coded as IDENT1100 and IDENT1300 at the AFOSR-IFP-Stanford Conference 1968, have been chosen . The first one is the flow in divergent channel, and the velocity distribution of the inviscid potential flow is shown in the following Fig. (3.1.a) and velocity gradient distribution in Fig. (3.1.b). For the edge of boundary layer the momentum equation is reduced to the form

$$U_e \frac{dU_e}{dx} = -\frac{dp_e}{dx}. \tag{3.33}$$

It is evident that this is mild adverse pressure gradient flow ($dp/dx > 0$).

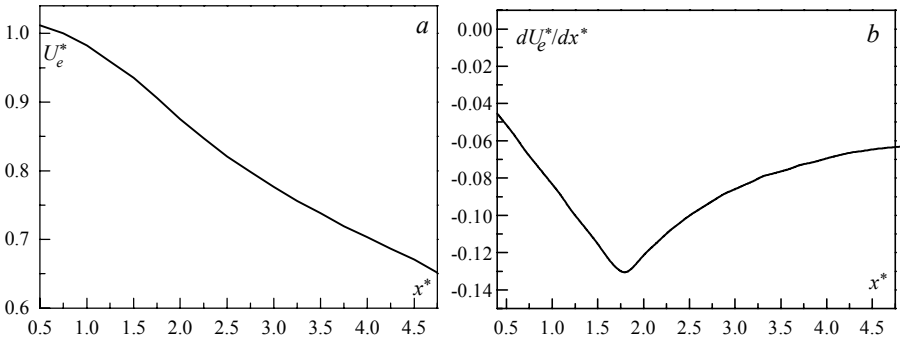

Fig. 3.1. Potential velocity and velocity gradient distribution for IDENT 1100

The results of the numerical solution of the equation (3.11) with boundary conditions (3.14) by using turbulent models (3.28) (3.30) (3.32) for the flow coded as IDENT 1100 are shown in the Fig.3.2 (*a-f*). The values of the functions F,F',F'' are shown in Fig 3.2.(*a-c*) for five different cross-sections; - (x^*=0.78); 2 - (x^* = 1.78); 3 - (x^* = 2.78); 4 - (x^* = 3.78); 5 - (x^* = 4.38). These values are obtained by the Cebecci-Smith turbulence model (3.30) and are in very good agreement with experimental values quoted in Coles & Hirst (1968, p.56).

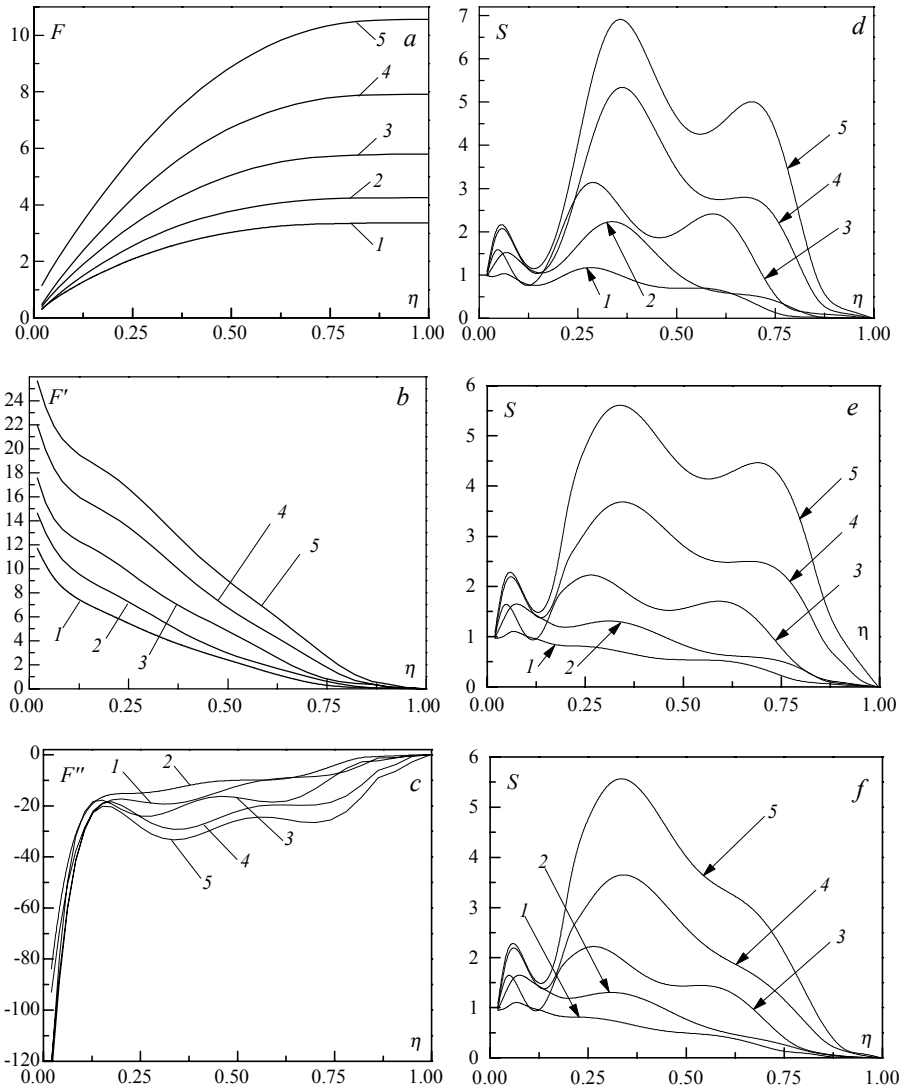

Fig. 3.2. The distribution of the functions F, F', F'' for five cross-sections, as well the nondimensional turbulent stress distribution $S(x^*,\eta)$ for three different turbulent models: *d*-Michell (1968), *e*-Cebecci & Smith (1974), *f*-Clauser (1956), for the flow coded as IDENT 1100 ($dp/dx>0$)

In the Fig. 3.2. (*d-f*) the nondimensional turbulent stress, obtained by three different turbulent models (3.28) (3.30) (3.32), has been shown for five different cross sections at same distances as in Fig.3.2 (*a-c*). It is obvious that for the mild adverse pressure distribution the values of turbulent stress τ_t over the different cross-sections are several times grater than the viscous stress at the wall τ_w, in other words, than the total shear stress in the viscous wall layer, since $S > 1$ for almost all values η and x^* in fully

turbulent defect layer.

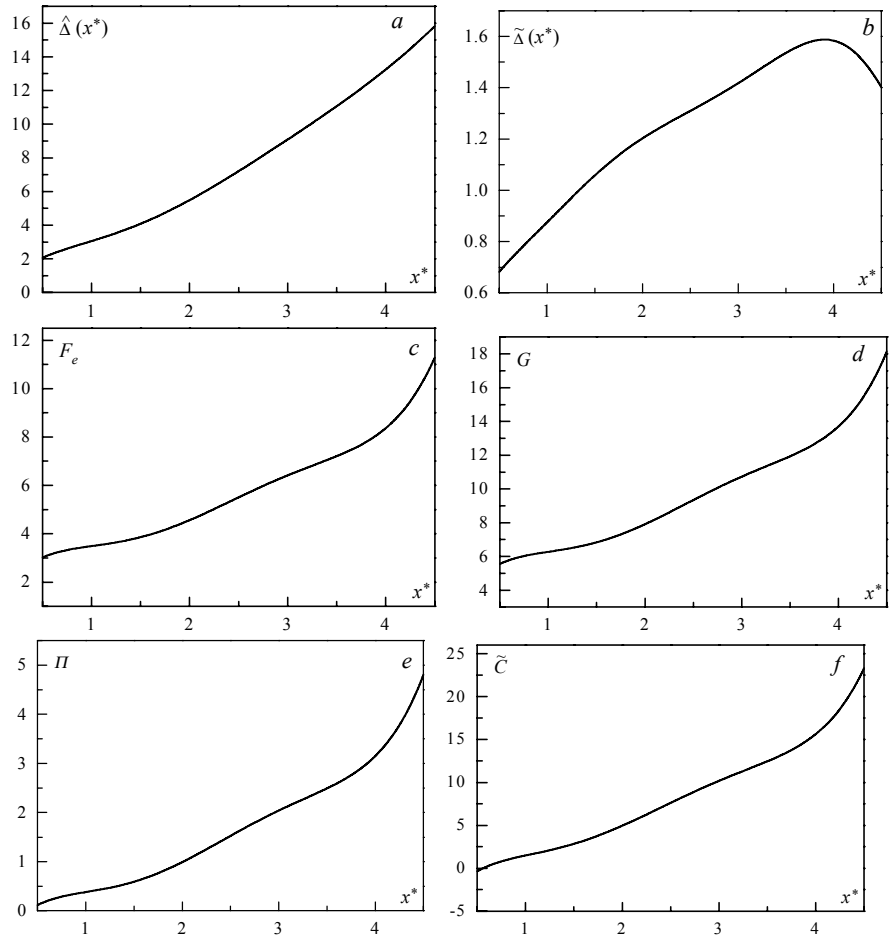

Fig. 3.3. The global values distribution of turbulent boundary layer for the flow coded as IDENT 1100

In the Fig3.3 . are shown the global values distributions of turbulent boundary layer $F_e(x^*)$, $G(x^*)$, $\Pi(x^*)$, $\tilde{C}(x^*)$, $\tilde{\Delta}(x^*)$ and $\hat{\Delta}(x^*)$. These values have been obtained by using Cebeci-Smith turbulence model (3.30), and are independent of Reynolds number. They are calculated only once for the given flow geometry, i.e. for the given pressure distribution. This values can be used for calculation of skin friction c_f by using the equation (3.26) for any value of Reynolds number if the Reynolds number high enough is ($Re_\theta > 6000$). Values obtained by the other turbulent models can be found in Jovanovic (1998).

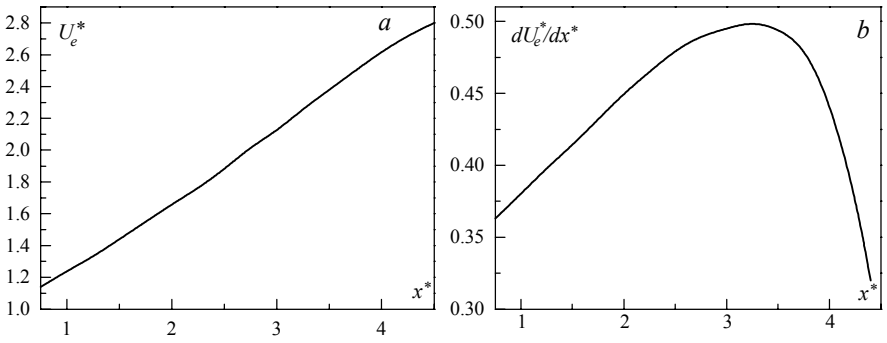

Fig. 3.4. Potential velocity and velocity gradient distribution forIDENT 1300

In the Fig.3.4 are sketched the velocity and velocity gradient distribution of the outer inviscid flow for the flow coded as IDENT 1300. It is evident from the figure that it is the mild favourable pressure gradient $dp/dx < 0$, in the other words, it is the case of longitudinal accelerated turbulent boundary layer.

In the Fig.3.5 are shown the results of the numerical solution of the equations (3.11) with boundary conditions (3.14) by using turbulent models (3.28) (3.30) (3.32). The values of the functions F,F',F'' are shown in Fig3.4.(*a-c*) for five different cross-sections; - (x^*=0.78); 2 - (x^* = 1.78); 3 - (x^* = 2.78); 4 - (x^* = 3.78); 5 - (x^* = 4.38). These values of the functions F,F',F'' are obtained by the Cebecci-Smith turbulence model (3.30) and are also the closest values to the experimental ones of all three turbulent models (the maximal deviation is under 2%).

Comparing the values of $F(x^*,\eta)$ in the Fig.3.2a and in the Fig3.5a, it is evident that the values of $F(x^*,\eta)$for the flow with $dp/dx > 0$ are grater than the ones for the case of $dp/dx < 0$. The same can be concluded from the Fig.3.2b and the Fig.3.5b, however the values of $F'(x^*,\eta)$ in the Fig.3.2b are the grater at the smaller values of η ($\eta < 0.75$) than the values in the Fig.3.5b. The similar situation is with the function $F''(x^*,\eta)$. The variation of this function is much more noticeable at the case of $dp/dx > 0$ than at the case of $dp/dx<0$. This fact has for consequence the smaller values of nondimensional turbulent stress $S(x^*,\eta)$ in the case of $dp/dx < 0$. In the Fig.3.5(*d-f*) are sketched the variations of the function $S(x^*,\eta)$ for the three algebraic turbulent models. The Clauser and Cebeci-Smith model yield almost the same distribution of the function $S(x^*,\eta)$. Only the Michell model shows some discrepancies in comparison with the forehead mentioned models. This model yields very good results for the flow with $dp/dx > 0$ (deviations of the numerical results were less than 7% from experimental ones), but for the case of $dp/dx < 0$, these deviations were larger (more details in Jovanovic 1998).

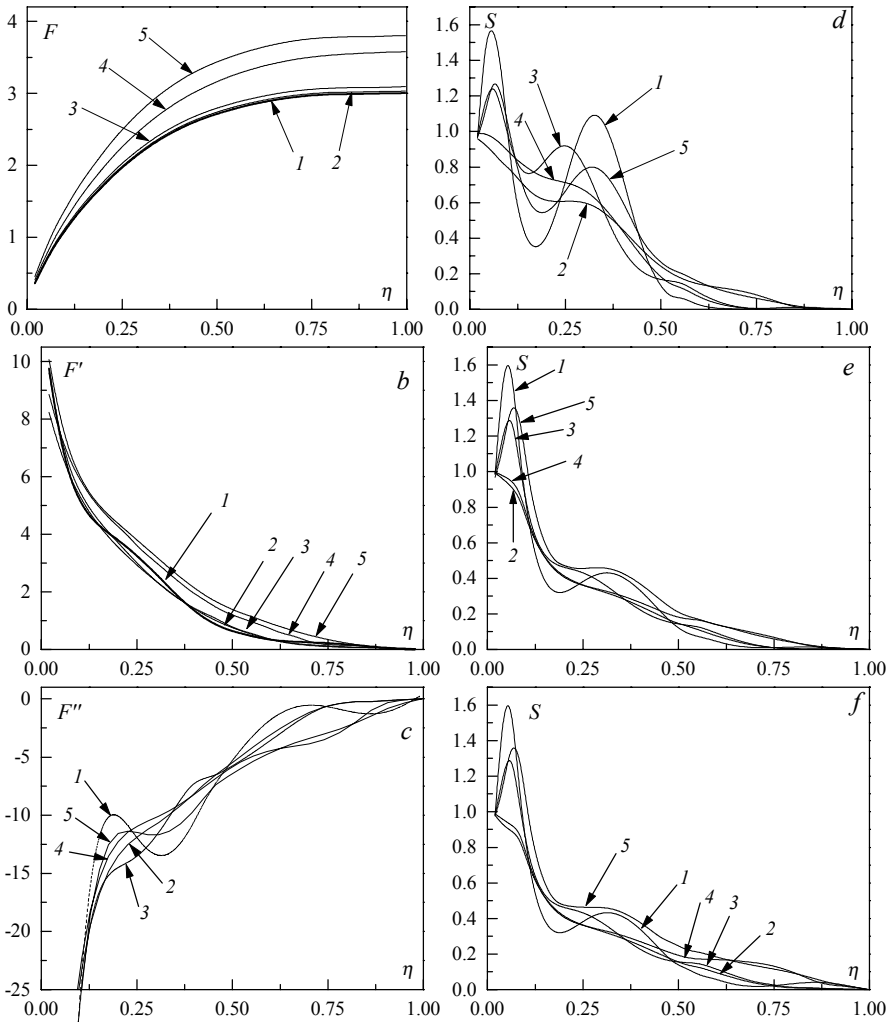

Fig. 3.5. The distribution of the functions F, F', F'' for five cross-sections, as well the nondimensional turbulent stress distribution $S(x^*,\eta)$ for three different turbulent models: *d*-Michell (1968), *e*-Cebecci & Smith (1974), *f*-Clauser (1956), for the flow coded as IDENT 1300 ($dp/dx<0$)

The global values distribution of turbulent boundary layer for the flow IDENT 1300 is shown in the Fig.3.6. It turns out that the distributions of the $F_e(x^*)$, $G(x^*)$, $\Pi(x^*)$, are mutual very similar not only in the Fig.6 (*c*,*d*,*f*) but also in Fig.5(*c*,*d*,*f*). The values of the function $F_e(x^*)$, $\Pi(x^*)$, $\widetilde{C}(x^*)$, $\widetilde{\Delta}(x^*)$ and $\hat{\Delta}(x^*)$ are grater for the flow with $dp/dx > 0$ than for the flow $dp/dx < 0$, unlike the function $G(x^*)$where the situation is opposite.

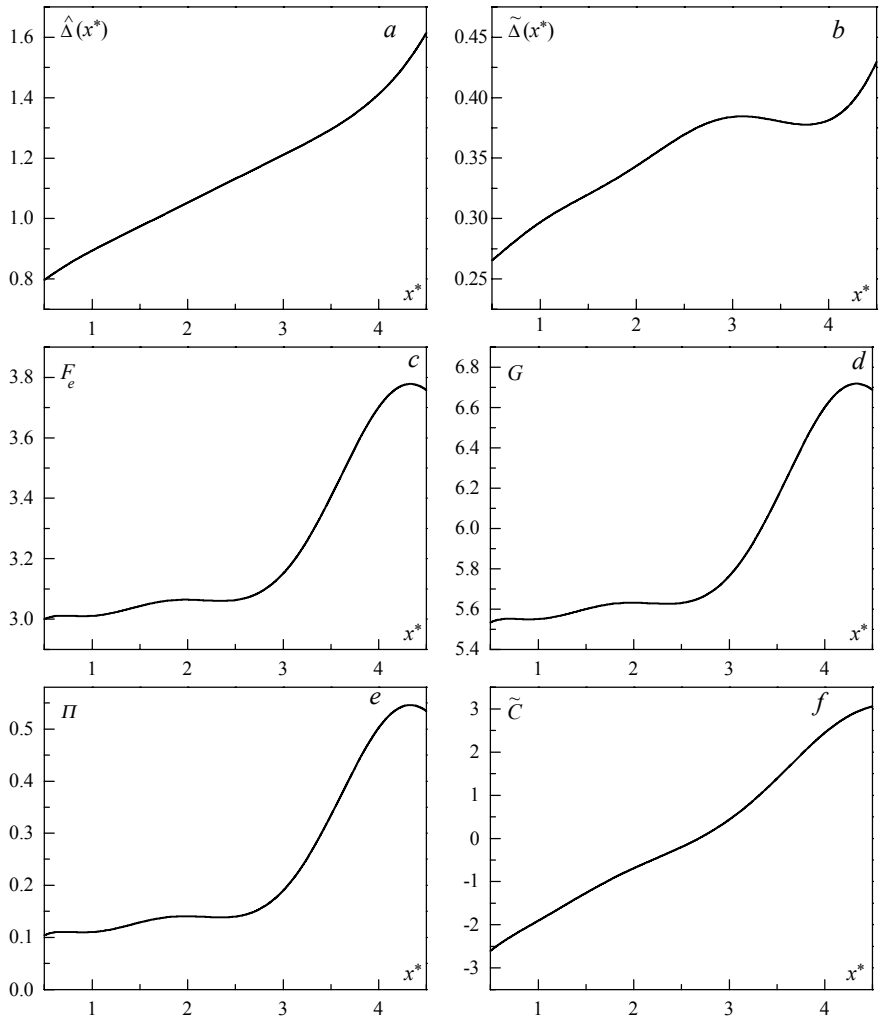

Fig. 3.6. The global values distribution of turbulent boundary layer for the flow coded as IDENT 1300

4. INDIRECT TURBULENCE MODEL: THE LAW OF THE WAKE

It is imortant to emphasis that on the basis of numerious experimental data *D*. Coles (1956) has suggested the following expression for the solution of $F'(x^*,\eta)$ defined by expression (3.3):

$$\frac{U_e(x)-\overline{U}}{u_\tau(x)} = F'(x,\eta) = \frac{1}{\kappa}\{\Pi(x)[2-W(\eta)]-\ln\eta\} \tag{4.1}$$

where $W(\eta)$ is wake funktion and $\Pi(x)$ is defined by the equation (3.18). This

represantation is known as *the law of the wake*. The three free parameters $\delta(x)$, $\tau(x)$ and $\Pi(x)$ are determined in such a way, that the measured velocity profiles are possibly best matched (indirect turbulence model). The wake function has the following boundary conditions:

$$W(0)=0,\ \ W'(0)=0,\ \ W(1)=2,\ \ W'(1)=0,\ \ \int_0^1 W(\eta)d\eta=1 \tag{4.2}$$

If the following wake function is chosen:

$$W(\eta)=1-\cos\pi\eta=2\sin^2\left(\frac{\pi}{2}\eta\right) \tag{4.3}$$

so that the values defined by the equations (3.17) and (3.18) now read:

$$F_e=\int_0^1 F'd\eta=\frac{1}{\kappa}(1+\Pi) \tag{4.4}$$

$$G(x)=\frac{1}{F_e\kappa^2}(2+3.179\Pi+1.5\Pi^2) \tag{4.5}$$

The results are altered only slightly if the wake function with power law is used $W(\eta)=2\eta^2(3-2\eta)$. The corrections of the law of the wake with improvements on the outer edge of boundary layer are undertaken by A.K.Lewkowicz (1982) and described in the work of J. Klauer (1989).

5. CONCLUSION

In the paper the global values of turbulent boundary layers coded as IDENT 1100 and IDENT 1300 on AFOSR-IFP-Stanford Conference 1968 have been obtained. It has been shown that it is needed to find global values of boundary layer that are independent of Reynolds number, and they can be later used for the calculation of skin friction, which is dependent on Reynolds number, not only for given Reynolds number for the Flows IDENT 1300 and IDENT 1100 but also for different Reynolds numbers, but for given nondimensional velocity and velocity gradient distribution (pressure distribution) of outer inviscid flow. The main goal of this paper was to test three different algebraic turbulent models, and to compare the values of $F(x,\eta)$, $F'(x,\eta)$, $F''(x,\eta)$, $S(x,\eta)$, with the available experimental data.The best agreement with experimental data for the flows coded as IDENT1300 and IDENT1100 has had Cebecci-Smith model, whose computational results agree very well with experimental data, and deviation is less than 2% for $F'(x,\eta)$.

REFERENCES:

1. Schlichting H. and K.Gersten, *Grenzschicht-Theorie*, Springer-Verlag, Berlin Heidelberg New York, 9.völlig neu bearbeitete und erweiterte Auflage, 1997.
2. Mellor G.L., *The large Reynolds number asymptotic theory of turbulent boundary layers*, Intern. Jour. of Engng. Sciences, Pergamon Press, 1972, vol.10, pp. 851-873

3. Keller H.B. and Cebeci T., *Accurate numerical methods for boundary-layer flows. II:two-dimensional turbulent flows*, AIAA Jouranal, 1972, vol.10, No.9, pp.1193-1199
4. Michell R., Quemard C., Durant R., *Hypothesis on the mixing length and application to the calculation of turbulent boundary layers*. Proceedings Computation of Turbulent Boundary Layers-1968. AFOSR-IFP-Stanford Conference, Vol. I, 195-207.
5. Clauser F.H., *The turbulent boundary layer*. Advances in Applied Mechanics, Vol.4, p.1-51
6. Cebeci T., Smith A.M.O., *Analysis of Turbulent Boundary Layers*, Academic Press, New York, 1974,
7. Coles D.E., Hirst E.A., *Computation of turbulent boundary layers -1968*-Proceedings, AFOSR-IFP-Stanford Conference, volume II, compiled data.
8. Jovanovic M., *The Steady, plane, turbulent boundary layer of incompressible fluid*, M.Sc. Thesis, Faculty of Mechanical Engineering, University of Nis, Yugoslavia, 1998
9. Coles D. (1956), *The law of the wake in the turbulent boundary layer*. J.Fluid Mech., Vol.1 191-226
10. Lewkowicz A.K.(1982), *An improved universal wake function for turbulent boundary layers and some of its consequences*. Z.Flugwiss.Weltraumfor.,Bd.6,261-266
11. Klauer J. (1989), *Computation of plane turbulent shear layers with separation and recirculation at high Reynolds numbers*, Ph.D. thesis, Ruhr-University Bochum.
12. Gersten K.,Vieth D. (1995), *Calculation of attached boundary layers at high Reynolds numbers*. The paper on the occasion of 70.Birthday of prof.J.Siekmann, University of Essen, Germany, proceedings 129-140.

PRORAČUN NEKOMPRIMOVANOG GRANIČNOG SLOJA SA RAZLIČITIM GRADIJENTIMA PRITISKA PRI VIŠIM REYNOLDS-OVIM BROJEVIMA

Miloš M. Jovanović

Pokazano je da se turbulentni granični sloj sastoji iz dva sloja: potpuno turbulentnog sloja (defektnog sloja) i viskoznog sloja uz zid. Proračun se može ograničiti na potpuno turbulentni sloj (defektni sloj), čije jednačine su nezavisne od Reynolds-ovog broja. Odgovarajući granični uslovi slede iz uslova spajanja sa spoljašnjim neviskoznim strujanjem (na spoljašnoj ivici $y=\delta$) i sa strujanjem viskoznog sloja uz zid (u preklapajućem sloju $y\approx\delta_v$) respektivno. Struktura zakona o koeficijentu trenja je nezavisna od modela turbulencije. Tri algebarska modela su korišćena u proračunu globalnih vrednosti defektnog sloja. Raspodela brzine i napona unutar viskoznog sloja uz zid pri velikim Reynods-ovim brojevima ima univerzalni oblik ako je Reynolds-ov broj dovoljno veliki ($Re_\theta > 6000$).

Na ovaj način pri zadatoj raspodeli brzine potencijalnog strujanja na spoljašnjoj ivici graničnog sloja potrebno je sprovesti samo jedan proračun. Uticaj Reynolds-ovog broja se uzima u obzir tek pri proračunu lokalnog koeficijenta trenja, koji se određuje iz uslova spajanja sa strujanjem u viskoznom sloju uz zid. Globalne karakteristike turbulentnog graničnog sloja mogu se dobiti numeričkim rešenjem jednačine defektnog sloja turbulentog graničnog sloja.